



PERFORMANCE-BASED DESIGN OPTIMIZATION OF STEEL MOMENT FRAMES

S. Gholizadeh^{1,*}, R. Kamyab² and H. Dadashi¹

¹*Department of Civil Engineering, Urmia University, Urmia, Iran*

²*The Iranian Academic Center for Education, Culture and Research, Kerman, Iran*

ABSTRACT

This study deals with performance-based design optimization (PBDO) of steel moment frames employing four different metaheuristics consisting of genetic algorithm (GA), ant colony optimization (ACO), harmony search (HS), and particle swarm optimization (PSO). In order to evaluate the seismic capacity of the structures, nonlinear pushover analysis is conducted (PBDO). This method is an iterative process needed to meet code requirements. In the PBDO procedure, the metaheuristics minimize the structural weight subjected to performance constraints on inter-story drift ratios at various performance levels. Two numerical examples are presented demonstrating the superiority of the PSO to the GA, ACO and HS metaheuristic algorithms.

Received: 15 February 2013; Accepted: 5 May 2013

KEY WORDS: structural optimization; metaheuristic; performance-based design; nonlinear pushover analysis; steel structure;

1. INTRODUCTION

In the seismic design process of a structural system the number of parameters which affect the structural performance and consequently the design is usually large. In this case, recognizing that the current design is the best solution or still there is room for finding cost-efficient solutions satisfying design code requirements is a difficult task. In the face of increase in price of materials, finding cost-efficient structural designs, with improved performance, is one of the major concerns in the field of structural engineering. In order to

*Corresponding author: S. Gholizadeh, Department of Civil Engineering, Urmia University, Urmia, Iran

†E-mail address: s.gholizadeh@urmia.ac.ir

achieve this purpose, structural optimization methodologies have been developed during the last decades. The performance-based design (PBD) of steel structures in the framework of structural optimization is a topic of growing interest [1-6]. In the PBD approach, nonlinear analysis procedures are efficiently employed to evaluate the nonlinear seismic responses of structures. Pushover analysis is a simplified, static nonlinear procedure in which a predefined pattern of earthquake loads is applied incrementally to framework structures until a plastic collapse mechanism is reached. This analysis method generally adopts a lumped-plasticity approach that tracks the spread of inelasticity through the formation of nonlinear plastic hinges at the frame element's ends during the incremental loading process [7].

In PBD design codes, such as FEMA-356 [8], performance ratings are divided into three levels: Immediate Occupancy (IO), Life Safety (LS) and Collapse Prevention (CP) [8]. The IO level implies very light damage with minor local yielding and negligible residual drifts. In the Life Safety (LS) level, the structure tolerates severe damage, but it remains safe for the occupants to evacuate the building. The CP level is associated with extensive inelastic distortion of structural members and an increase in load or deflection results in collapse of the structure. The PBD methods tend to consider the nonlinear seismic response of structures. These methods directly address inelastic deformations to identify the levels of damage during severe seismic events. A nonlinear analysis tool is required to evaluate earthquake demands at the various performance levels. Pushover analysis is widely adopted as the effective tool for such nonlinear analysis because of its simplicity compared with dynamic nonlinear procedures. The purpose of the nonlinear static pushover analysis is to assess structural performance in terms of strength and deformation capacity globally as well as at the element level. The outcome of pushover analysis is the inelastic capacity curve of the structure.

In order to replace the traditional PBD process with an automatic advanced procedure for seismic design of structures, optimization algorithms can be effectively used. In this case, pushover analysis can be incorporated in a structural optimization strategy to evaluate the structural performance at the various performance levels. In the last years, many researches have been done in the field of performance-based design optimization (PBDO) of structures. However, metaheuristics have been employed in a few numbers of these researches. In this work, the well-known genetic algorithm (GA) [9], ant colony optimization (ACO) [10], harmony search (HS) [11] and particle swarm optimization (PSO) [12] metaheuristics are employed to achieve PBDO of steel moment-resisting frames.

Two six and twelve story planar steel frame structures are optimized for various performance levels using GA, ACO, HS and PSO metaheuristics and the results are compared. The results indicate that PSO converges to better solutions compared with the other algorithms.

2. PERFORMANCE-BASED DESIGN OPTIMIZATION PROCESS

In PBD frameworks, a performance objective is defined as a given level of performance for a specific hazard level. To define a performance objective, at first the level of structural

performance should be selected and then the corresponding seismic hazard level should be determined. In the present work, immediate occupancy (IO), life safety (LS) and collapse prevention (CP) performance levels are considered according to FEMA-356. Each objective corresponds to a given probability of being exceeded during 50 years. A usual assumption [2] is that the IO, LS and CP performance levels correspond respectively to a 20%, 10% and 2% probability of exceedance in 50 year period. In this study, the mentioned hazard levels are considered.

In this work, the nonlinear static pushover analysis is utilized to quantify seismic induced nonlinear response of structures. Among various methods of static pushover analyses, the displacement coefficient method [8] procedure is adopted to evaluate the seismic demands on building frameworks under equivalent static earthquake loading. In this method the structure is pushed with a specific distribution of the lateral loads until the target displacement is reached. The target displacement can be obtained from the FEMA-356 as follows:

$$\delta_t = C_0 C_1 C_2 C_3 S_a \frac{T_e^2}{4\pi^2} g \tag{1}$$

where C_0 relates the spectral displacement to the likely building roof displacement; C_1 relates the expected maximum inelastic displacements to the displacements calculated for linear elastic response; C_2 represents the effect of the hysteresis shape on the maximum displacement response and C_3 accounts for P-D effects. T_e is the effective fundamental period of the building in the direction under consideration; S_a is the response spectrum acceleration corresponding to the T_e .

In this work, the OPENSEES [13] platform is utilized to conduct the pushover analyses.

In a sizing structural optimization problem, the aim is usually to minimize the weight of the structure under some behavioural constraints. For a steel frame structure consisting of ne members that are collected in ng design groups, if the variables associated with each design group are selected from a given profile list of steel sections, a discrete optimization problem can be formulated as follows:

$$\text{Minimize: } w(X) = \sum_{i=1}^{ng} \rho_i A_i \sum_{j=1}^{nm} L_j \tag{2}$$

$$\text{Subject to: } g_k(X) \leq 0, \quad k=1,2,\dots,nc \tag{3}$$

$$X = \{x_1 \quad x_2 \quad \dots \quad x_i \quad \dots \quad x_{ng}\}^T \tag{4}$$

where x_i is an integer value expressing the sequence numbers of steel sections assigned to i th group; w represents the weight of the frame, ρ_i and A_i are weight of unit volume and cross-sectional area of the i th group section, respectively; nm is the number of elements collected in the i th group; L_j is the length of the j th element in the i th group; $g_k(X)$ is the k th behavioral constraint. In the present study, design variables are selected from W-shaped sections found in the AISC design manual [14].

In this study, the constraints of the optimization problem are handled using the concept of exterior penalty functions method (EPFM) [15]. In this case, the pseudo unconstrained objective function is expressed as follows:

$$\Phi(X, r_p) = w(X) \left(1 + r_p \sum_{k=1}^{nc} (\max\{0, g_k\})^2 \right) \quad (5)$$

where Φ and r_p are the pseudo objective function and positive penalty parameter, respectively.

3. METAHEURISTIC ALGORITHMS

The metaheuristics due to their high potential for simple computer implementation are now emerged as one of the most practical approaches for solving many complex problems. However, there are several newly developed metaheuristics, genetic algorithm (GA), ant colony optimization (ACO), harmony search (HS) and particle swarm optimization (PSO) are the most popular metaheuristics [16] and many successful application of them have been reported in literature. In the present work, standard versions of these metaheuristic algorithms are considered for implementation of PBDO of steel structures and their basic concepts are briefly described below.

3.1 Genetic Algorithm

A simple GA proceeds by randomly generating an initial population. The next generation is evolved from this population by performing reproduction, crossover, and mutation operations. Reproduction operator reproduces the next generation based on the statistics of current population. In this way, the weak designs are removed and the strong ones are transformed to the next generation. In the crossover operation, two members of the population are randomly selected, as parents, and two new offsprings are produced by exchanging a part of parents' string at a randomly selected position with a specified probability of crossover. Finally, with a probability of mutation, certain digits of the chromosomes are altered. In this way, the population takes its final form in the current generation. After several generations, the best individual of the population is considered as the final solution of the algorithm. The stochastic nature of the method and using a population of design points in each generation usually give rise to the global optimum. The full details of the method can be found in the literature [16].

Up to now standard GA and its improved versions have been extensively employed by researchers to efficiently tackle the complex problems in the area of structural engineering. A number of such applications may be found in [17-18].

3.2 Ant Colony Optimization

ACO is based on the cooperative behaviour of real ant colonies, which are able to find the shortest path from their nest to a food source. The ACO process can be explained as follows. The ants start at the home node, travel through the various nodes from the first node to the last

node, and end at the destination node in each iteration. Each ant can select only one node in each layer in accordance with the state transition rule [19]. An ant k , when located at node i , uses the pheromone trail τ_{ij} to compute the probability of choosing j as the next node:

$$P_{ij}^{(k)} = \begin{cases} \frac{\tau_{ij}^\alpha}{\sum_{j \in N_i^{(k)}} \tau_{ij}^\alpha} & \text{if } j \in N_i^{(k)} \\ 0 & \text{if } j \notin N_i^{(k)} \end{cases} \quad (6)$$

where α denotes the degree of importance of the pheromones and $N_i^{(k)}$ indicates the set of neighbourhood nodes of ant k when located at node i .

The neighbourhood of node i contain all the nodes directly connected to node i except the predecessor node. This will prevent the ant from returning to the same node visited immediately before node i . An ant travels from node to node until it reaches the destination node. Before returning to the home node, the k th ant deposits an amount of pheromone on arcs it has visited. After all the ants return to the nest, the pheromone information is updated in order to increase the pheromone value associated with good or promising paths. The updating is achieved as follows:

$$\tau_{ij} = (1 - \rho)\tau_{ij} + \Delta\tau_{ij}^{(k)} \quad (7)$$

$$\Delta\tau_{ij}^{(k)} = \frac{Q}{L_k} \quad (8)$$

where $\rho \in (0, 1]$ is the pheromone decay factor; $\Delta\tau_{ij}^{(k)}$ is the amount of pheromone deposited on arc ij by the best ant k . also, Q is a constant and L_k is the length of the path traveled by the k th ant.

When more paths are available from the nest to a food source, a colony of ants will be able to exploit the pheromone trails left by the individual ants to discover the shortest path from the nest to the food source and back [19]. In fact, ACO simulates the optimization of ant foraging behaviour.

During the last years some applications of ACO in the field of structural engineering have been reported in [20-22].

3.3 Harmony Search Algorithm

The harmony search (HS) algorithm is based on the musical performance process that achieves when a musician searches for a better state of harmony. In the process of musical production a musician selects and brings together number of different notes from the whole notes and then plays these with a musical instrument to find out whether it gives a pleasing harmony. The musician then tunes some of these notes to achieve a better harmony [16].

For implementation of HS, at first a harmony memory (HM), the harmony considering rate (HMCR), the pitch adjusting rate (PAR) and the maximum number of searches should be specified. To improvise new HM, a new harmony vector is generated. Thus the new value of

the i th design variable can be chosen from the possible range of i th column of the HM with the probability of HMCR or from the entire possible range of values with the probability of 1-HMCR as follows:

$$x_i^{\text{new}} = \begin{cases} x_i^j \in \{x_i^1, x_i^2, \dots, x_i^{\text{HMS}}\}^T & \text{with the probability of HMCR} \\ x_i \in \Delta_i & \text{with the probability of } (1 - \text{HMCR}) \end{cases} \quad (9)$$

where Δ_i is the set of the potential range of values for i th design variable.

Pitch adjusting is performed only after a value has been chosen from the HM as follows:

$$\text{pitch adjustment of } x_i^{\text{new}} ? \begin{cases} \text{Yes} & \text{with the probability of PAR} \\ \text{No} & \text{with the probability of } (1 - \text{PAR}) \end{cases} \quad (10)$$

If the pitch-adjustment decision for x_i^{new} is "Yes", then a neighbouring value with the probability of $\text{PAR} \times \text{HMCR}$ is taken for it as follows:

$$x_i^{\text{new}} \leftarrow \begin{cases} x_i^{\text{new}} \pm u(-1, +1) \times bw & \text{with the probability of } \text{PAR} \times \text{HMCR} \\ x_i^{\text{new}} & \text{with the probability of } \text{PAR} \times (1 - \text{HMCR}) \end{cases} \quad (11)$$

where $u(-1, +1)$ is a uniform distribution between -1 and +1; also bw is an arbitrary distance bandwidth for the continuous design variables.

If x_i^{new} is better than the worst vector in the HM, the new harmony is substituted by the existing worst harmony.

Computational merits of HS for tackling complex structural optimization problems have been demonstrated in many researches such as those of reported in [23-25].

3.4 Particle Swarm Optimization

The particle swarm optimization (PSO) is based on the social behavior of animals such as fish schooling, insect swarming and bird flocking. The PSO has been proposed to simulate the graceful motion of bird swarms as a part of a socio-cognitive study.

The PSO involves a number of particles, which are randomly initialized in the search space. These particles are referred to as swarm. Each particle of the swarm represents a potential solution of the optimization problem. The particles fly through the search space and their positions are updated based on the best positions of individual particles and the best of the swarm in each iteration. The objective function is evaluated for each particle at each grid point and the fitness values of particles are obtained to determine the best position in the search space. In iteration k , the swarm is updated using the following equations:

$$V_i^{k+1} = \omega^k V_i^k + c_1 r_1 (P_i^k - X_i^k) + c_2 r_2 (P_g^k - X_i^k) \quad (12)$$

$$X_i^{k+1} = X_i^k + V_i^{k+1} \tag{13}$$

where X_i and V_i represent the current position and the velocity of the i th particle, respectively; P_i is the best previous position of the i th particle ($pbest$) and P_g is the best global position among all the particles in the swarm ($gbest$); r_1 and r_2 are two uniform random sequences generated from interval $[0, 1]$; c_1 and c_2 are the cognitive and social scaling parameters, respectively. The inertia weight used to discount the previous velocity of particle preserved is expressed by ω .

Due to the importance of ω in achieving efficient search behavior the updating criterion can be taken as follows:

$$\omega = \omega_{max} - \frac{\omega_{max} - \omega_{min}}{k_{max}} . k \tag{14}$$

where ω_{max} and ω_{min} are the maximum and minimum values of ω , respectively. Also, k_{max} , and k are the numbers of maximum iterations and present iteration, respectively.

Standard PSO is more efficient, requiring fewer number of function evaluations compared with other robust design optimization methods [26].

In the field of structural engineering many successful application of PSO have been reported in literature. A number of such applications can be found in [27-30].

4. ANALYSIS AND DESIGN OF STEEL FRAMES

In this study, two types of constraints are checked during the optimization process. The first type includes the checks of each structural element for gravity loads. In this case, the following load combination is considered:

$$Q_G^{Type1} = 1.2Q_D + 1.6Q_L \tag{15}$$

where Q_D and Q_L are dead and live loads, respectively.

Each structural element should satisfy the following constraints for the non-seismic load combinations according to the LRFD-AISC [14] code.

$$\text{for } \frac{P_u}{\phi_c P_n} < 0.2; \frac{P_u}{2\phi_c P_n} + \left(\frac{M_{ux}}{\phi_b M_{nx}} + \frac{M_{uy}}{\phi_b M_{ny}} \right) - 1 \leq 0 \tag{16}$$

$$\text{for } \frac{P_u}{\phi_c P_n} \geq 0.2; \frac{P_u}{\phi_c P_n} + \frac{8}{9} \left(\frac{M_{ux}}{\phi_b M_{nx}} + \frac{M_{uy}}{\phi_b M_{ny}} \right) - 1 \leq 0 \tag{17}$$

where P_u is the required strength (tension or compression); P_n is the nominal axial strength

(tension or compression); ϕ_c is the resistance factor; M_{ux} and M_{uy} are the required flexural strengths in the x and y directions; respectively; M_{nx} and M_{ny} are the nominal flexural strengths in the x and y directions; and ϕ_b is the flexural resistance reduction factor ($\phi_b = 0.9$).

If the first type constraints are not satisfied then the candidate design is rejected, else a nonlinear pushover analysis based on the displacement coefficient method is performed in order to estimate the maximum inter-story drift ratios at various performance levels. In nonlinear static pushover analysis, the lateral load distribution in the height of the frame is defined as follows [31]:

$$P_s = V_b \left(\frac{G_s H_s^k}{\sum_{m=1}^{ns} G_m H_m^k} \right) \quad (18)$$

where P_s = lateral load applied at story s ; V_b = base shear; H_s , H_m = height from the base of the building to stories s and m , respectively; G_s , G_m = seismic weight for story level s and m , respectively; k = constant number determined by the period and as well as [3], in this paper, k is also chosen to be 2.

The following component gravity force is considered for combination with the seismic loads [8]:

$$Q_G^{\text{Type2}} = 1.1(Q_D + Q_L) \quad (19)$$

The lateral inter-story drift constraints at various performance levels can be expressed as follows:

$$g_k^i(X) = \frac{\theta_k^i}{\theta_{all}^i} - 1 \leq 0, \quad i = \text{IO; LS; CP}, \quad k = 1, 2, \dots, ns \quad (20)$$

where θ_k^i and θ_{all}^i are respectively the k th story drift and its allowable value of a steel moment-resisting frame associated with i th performance level; ns is the number of stories.

In order to implement pushover analysis, the target displacement should be determined. To achieve this task, S_a should be calculated for the three performance levels. In this case three acceleration design spectra, which represent three different earthquake levels corresponding to 20%, 10%, and 2% probability of exceeding in a 50-year period, are taken as the basis for calculating the seismic loading for the three performance levels IO, LS, and CP, respectively. Without loss of generality, the calculation of spectral acceleration S_a^i for each design spectrum i can be expressed as:

$$S_a^i = \begin{cases} F_a S_s^i (0.4 + 3T/T_0) & \text{if } 0 < T \leq 0.2T_0^i \\ F_a S_s^i & \text{if } 0.2T_0^i < T \leq T_0^i \\ F_v S_1^i / T & \text{if } T > T_0^i \end{cases}, \quad i = \text{IO, LS, CP} \quad (21)$$

$$T_0^i = \frac{F_v S_1^i}{F_a S_s^i} \tag{22}$$

where T is the elastic fundamental period of the structure, which is computed here from structural modal analysis; S_s^i and S_1^i are the short-period and the first second-period response acceleration parameters, respectively. F_a and F_v are the site coefficient determined respectively from FEMA-273 [31], based on the site class and the values of the response acceleration parameters S_s^i and S_1^i , according to Table 1 [3].

Table 1. Performance level site parameters for site class of D

<i>Performance Level</i>	<i>Hazard Level</i>	S_s (g)	S_1 (g)	F_a	F_v
IO	20% / 50-years	0.658	0.198	1.27	2.00
LS	10% / 50-years	0.794	0.237	1.18	1.92
CP	2% / 50-years	1.150	0.346	1.04	1.70

5. NUMERICAL RESULTS

Two planar steel frames are optimized in this section. The frames are assumed to have rigid connections and fixed supports. The sections of all members are assumed to be selected from the 267 W-shaped sections from the AISC database. The value of the modulus of elasticity is 210 GPa and of the yield stress is 235 MPa. The constitutive law is bilinear with pure strain hardening slope equal to 3% of the elastic modulus. The dead load of $Q_D = 2500$ kg/m and live load of $Q_L = 1000$ kg/m are applied to the all beams.

For all the presented examples, the parameters of the metaheuristics are taken as follows: In the GA, crossover rate=0.9, mutation rate=0.001. In the ACO, $\alpha=1.0$, $\rho=0.2$, $Q=1.0$. In the HS, HMCR=0.9, PAR=0.25. And in the PSO, $c_1=1.0$, $c_2=3.0$, $\omega_{min}=0.4$, $\omega_{max}=0.9$.

In this paper, all of the required computer programs are coded in MATLAB [32]. Also for computer implementation a personal Pentium IV 3.0 GHz has been used.

The allowable values of inter-story drifts at the IO, LS and CP performance levels are taken as 0.7%, 2.5% and 5.0%, respectively.

Finally, in the numerical examples of this study, plastic hinge distributions in the optimum designs are presented at the IO, LS and CP performance levels. To achieve this, the yield rotation of beams and columns are calculated as follows according to FEMA-356:

$$\text{Beams: } \theta_y = \frac{ZF_{ye} l_b}{6EI_b} \tag{23}$$

$$\text{Columns: } \theta_y = \frac{ZF_{yc} l_c}{6EI_c} \left(1 - \frac{P}{P_{ye}}\right) \tag{24}$$

where E is modulus of elasticity; Z is plastic section modulus; F_{ye} is expected yield stress; I_b is beam moment of inertia; I_c is column moment of inertia; l_b is beam length; l_c is column length; P is axial force in the member at the target displacement and P_{ye} is expected axial yield force of the member..

5.1 Example 1: Six-story steel frame

The geometry and grouping details of the frame are shown in Figure 1. The frame has 3 beam and 6 column groups.

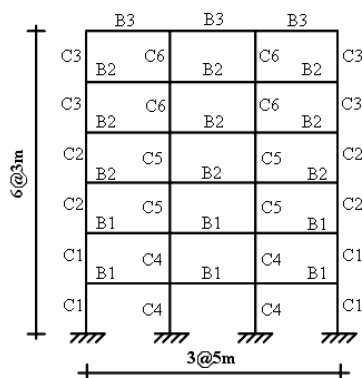


Figure 1. Six-story steel frame

The number of individuals in the population and the total number of generations considered in this example for all of the metaheuristics are 50 and 200, respectively. The results of optimization are presented in Table 2.

Table 2. Optimum designs of 6-story steel frame

Design Variables	Optimum Designs			
	GA	ACO	HS	PSO
C1	W24×55	W18×76	W24×55	W21×44
C2	W21×55	W16×40	W18×55	W18×35
C3	W21×50	W12×19	W18×46	W16×31
C4	W21×57	W18×76	W21×57	W18×55
C5	W21×55	W18×76	W21×55	W18×50
C6	W18×65	W21×55	W18×46	W18×35
B1	W21×44	W21×48	W21×44	W18×60
B2	W18×50	W18×40	W18×50	W18×46
B3	W18×46	W16×31	W14×34	W16×31
Weight (kg)	12296.54	11436.48	11353.69	10693.49

The results indicate that, among the employed metaheuristic algorithms, the PSO converges to the best solution. The structure found by HS is better than those of the ACO and GA while the optimal weight of the solution found by ACO is better in comparison with that of the GA. The convergence histories of GA, ACO, HS and PSO based optimization processes are given in Figure 2. It can be easily observed that PSO possesses better convergence behavior in comparison with other metaheuristics.

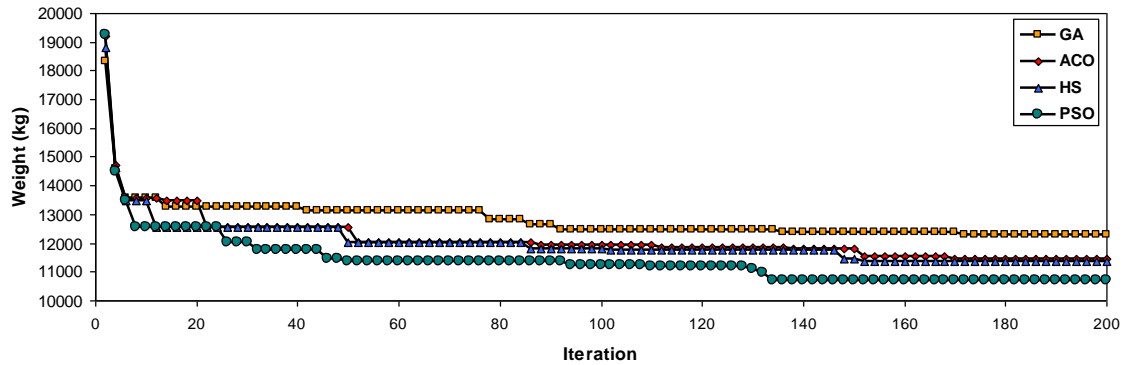


Figure 2. Convergence histories of GA, ACO, HS and PSO in PBDO of six-story frame

The drift profiles of the solution found by PSO, as the best solution, are shown at the IO, LS and CP performance levels in Figure 3. In this figure the vertical dashed lines denote the drift limit. The results show that the constraints associate with IO level dominates the designs.

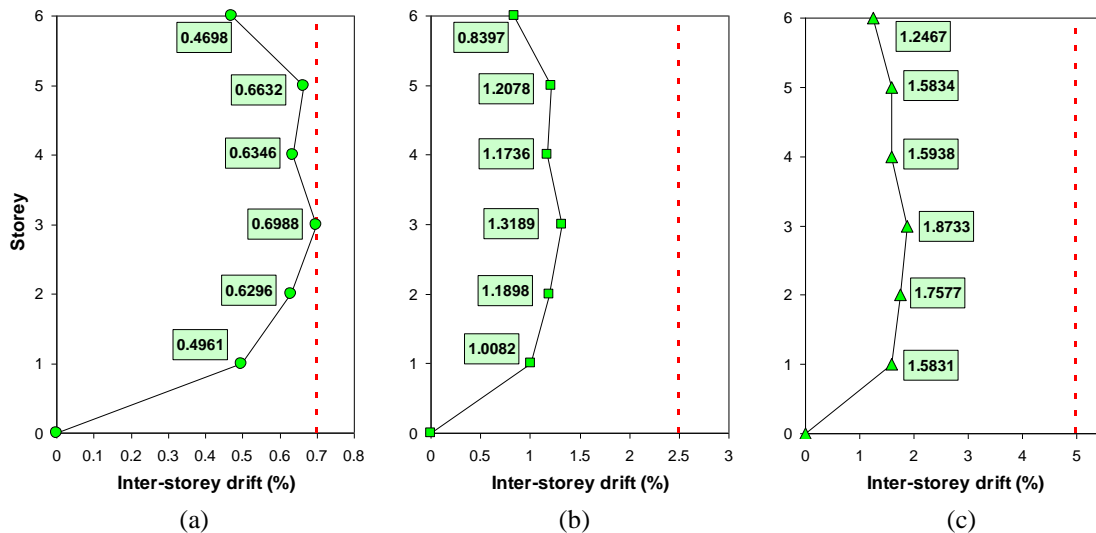


Figure 3. Story drifts profile of six-story frame at (a) IO, (b) LS and (c) CP levels

Plastic hinge distributions of the solution found by PSO under the pushover loading at the IO, LS and CP performance levels are shown in Figure 4.

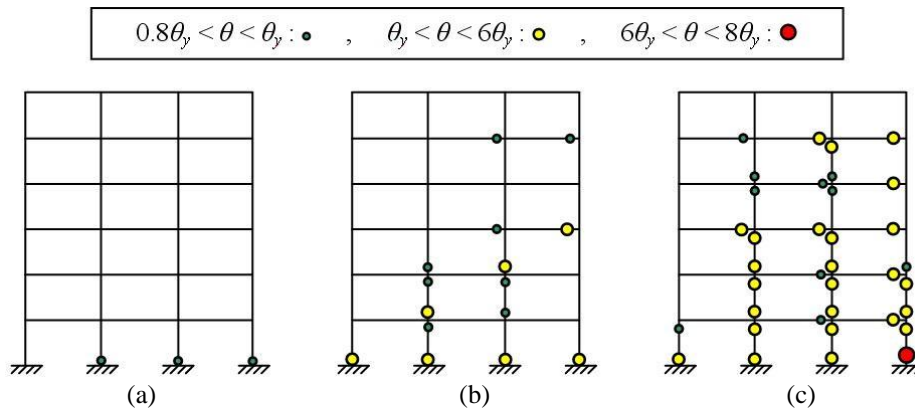


Figure 4. Plastic hinge distribution for six-story frame at (a) IO, (b) LS and (c) CP levels

No plastic hinge rotation is found to exceed the specified threshold of plastic rotation.

5.2 Example 2: Twelve-story steel frame

Figure 5 represents the geometry and grouping details of the frame. The frame has 6 beam and 18 column groups.

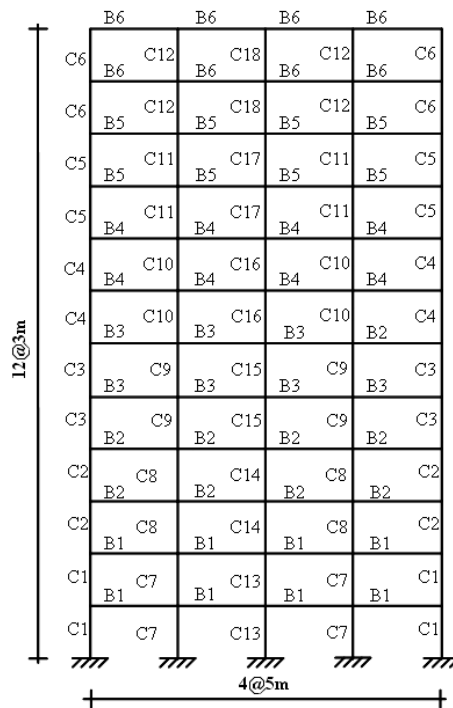


Figure 5. Twelve-story steel frame

In this example 75 particles are considered and the total number of generations is 300. The results of structural optimization are presented in Table 3.

Table 3. Optimum designs of twelve-story steel frame

Design Variables	Optimum Designs			
	GA	ACO	HS	PSO
C1	W24×68	W24×76	W24×76	W24×62
C2	W24×68	W24×76	W24×68	W21×50
C3	W24×68	W24×68	W16×89	W18×55
C4	W16×89	W16×89	W16×89	W21×44
C5	W16×50	W16×45	W16×45	W18×35
C6	W16×45	W14×26	W14×38	W16×26
C7	W24×94	W21×111	W21×111	W24×76
C8	W21×111	W21×101	W21×111	W24×68
C9	W21×68	W18×86	W16×89	W24×55
C10	W21×50	W21×50	W21×50	W21×55
C11	W18×50	W18×35	W18×35	W18×55
C12	W16×50	W14×38	W14×38	W16×26
C13	W24×94	W24×94	W24×94	W24×76
C14	W21×55	W21×55	W21×55	W24×68
C15	W21×55	W18×55	W18×55	W21×62
C16	W21×50	W18×46	W18×46	W21×55
C17	W18×46	W12×45	W12×45	W18×40
C18	W16×50	W10×30	W10×30	W14×26
B1	W21×55	W24×68	W21×48	W21×48
B2	W18×60	W21×55	W21×48	W21×48
B3	W21×50	W21×50	W21×44	W21×48
B4	W18×50	W21×48	W21×44	W18×40
B5	W16×50	W18×46	W18×46	W18×40
B6	W16×45	W14×38	W14×38	W14×26
Weight (kg)	36186.87	35491.61	33951.84	28747.07

The numerical results given in Table 3 demonstrate that, among the employed metaheuristic algorithms, PSO has the best computational performance. HS is better than the ACO and GA while the optimal design found by ACO is better than that of the GA. The convergence histories of GA, ACO, HS and PSO are given in Figure 6. It is obvious that the best convergence behavior associates with PSO.

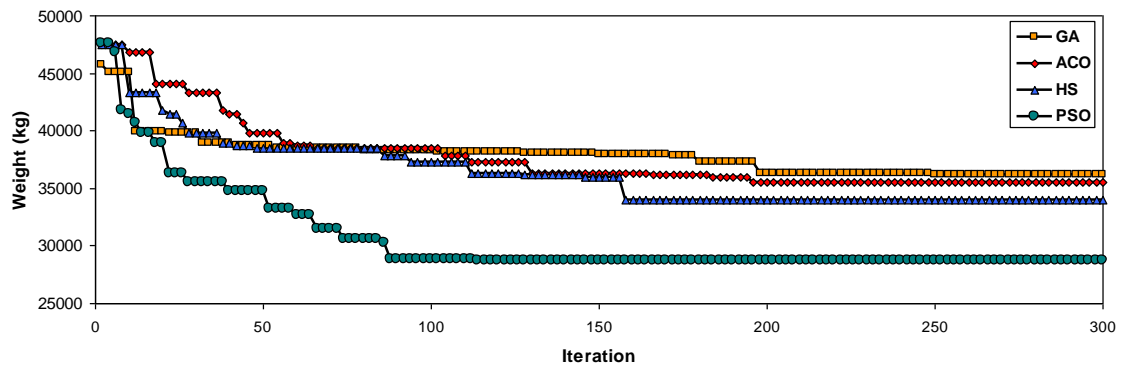


Figure 6. Convergence histories of GA, ACO, HS and PSO in PBDO of twelve-story frame

The inter-story drift profiles of the solution found by PSO, at the IO, LS and CP performance levels, are shown in Figure 7. In this figure the vertical dashed lines denote the drift limit. The results show that the constraints associate with IO level dominates the designs.

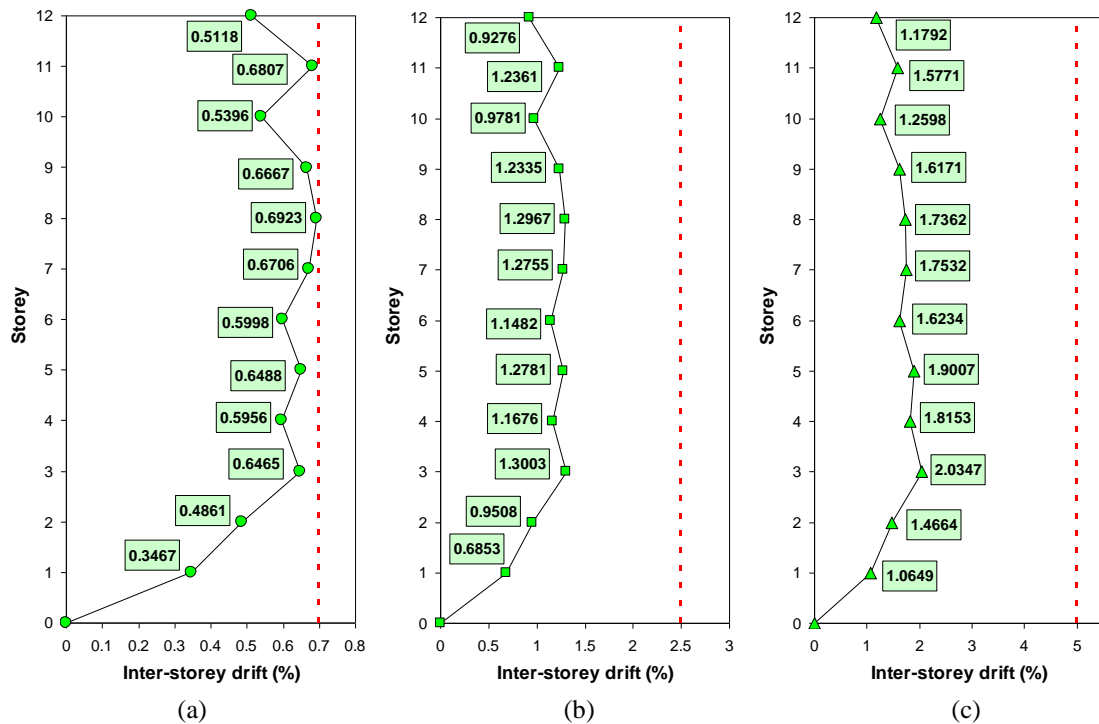


Figure 7. Story drifts profile of twelve-story frame at (a) IO, (b) LS and (c) CP levels

Plastic hinge distributions of the solution found by PSO under the pushover loading, at the IO, LS and CP performance levels, are depicted in Figure 8.

As well as the first example, no plastic hinge rotation is found to exceed the specified threshold of plastic rotations.

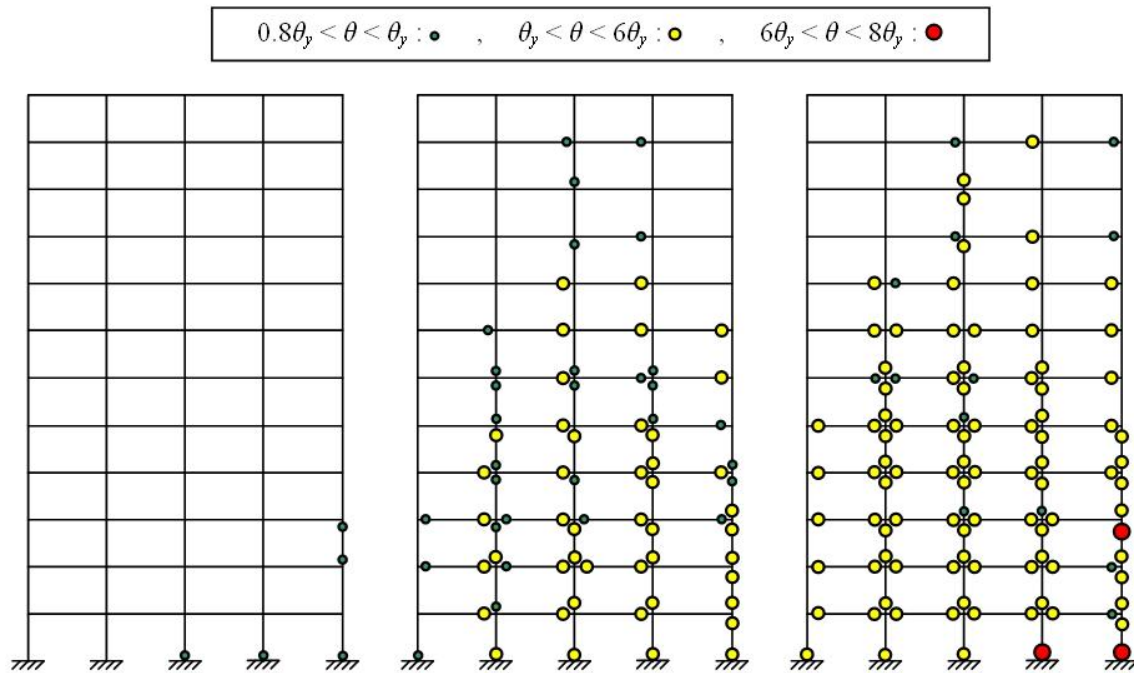


Figure 8. Plastic hinge distribution for 12-story frame at (a) IO, (b) LS and (c) CP levels

6. CONCLUSIONS

The present paper deals with PBDO of steel frames using metaheuristic optimization algorithms. Two types of design constraints are checked during the optimization process. In the first type, each structural element is checked to satisfy the AISD-LRFD constraints for the non-seismic load combinations. While the second type includes the check of inter-story drifts at IO, LS and CP performance levels according to the FEMA-356 provided constraints. Two numerical examples including a three-bay, six-story and a four-bay, twelve-story steel frames are presented. The optimization task is achieved using GA, ACO, HS and PSO metaheuristics and the results are compared. The numerical results demonstrate that in the first example, PSO finds a solution which is 5.81%, 6.49% and 13.04% lighter than those of the HS, ACO and GA, respectively. The results imply that the solution found by HS is better than those of the ACO and GA and the ACO possesses better performance in comparison with GA. In the second example, the optimal weight of PSO is 15.33%, 19.01% and 20.56% lighter than those of the HS, ACO and GA, respectively. It is observed again that the solution of HS is better than those of the ACO and GA. Also, ACO possesses better performance compared with GA. It can be concluded that the PSO provides results which are significantly better than those of the other metaheuristics. Also it is evident that in the large scale problems the improvement in optimal weight is considerable. Therefore, PSO can be effectively employed to design cost-efficient steel structures with desirable seismic performance.

REFERENCES

1. Kaveh A, Laknejadi K, Alinejad B. Performance-based multi-objective optimization of large steel structures, *Acta Mech*, 2012; **232**: 355–69.
2. Fragiadakis M, Lagaros ND. An overview to structural seismic design optimisation frameworks, *Comput Struct*, 2011; **89**: 1155–65.
3. Kaveh A, Farahmand Azar B, Hadidi A, Rezazadeh Sorochi F, Talatahari S. Performance-based seismic design of steel frames using ant colony optimization, *J Constr Steel Res*, 2010; **66**: 566–74.
4. Salajegheh E, Mohammadi A, Ghaderi Sohi S. Optimum performance based design of concentric steel braced frames, *the 14th World Conference on Earthquake Engineering*, Beijing, China, 2008.
5. Pan P, Ohsaki M, Kinoshita T. Constraint approach to performance-based design of steel moment-resisting Frames, *Eng Struct*, 2007; **29**: 186–94.
6. Fragiadakis M, Lagaros ND, Papadrakakis M. Performance-based multiobjective optimum design of steel structures considering life-cycle cost, *Struct Multidiscip Optim*, 2006; **32**: 1–11.
7. Zou XK, Chan CM. Optimal seismic performance-based design of reinforced concrete buildings using nonlinear pushover analysis, *Eng Struct*, 2005; **27**: 1289–302.
8. FEMA-356, Prestandard and commentary for the seismic rehabilitation of buildings. Federal Emergency Management Agency, Washington, DC, 2000.
9. Holland JH. *Adaptation in Natural and Artificial Systems*, Ann Arbor: University of Michigan Press, 1975.
10. Eberhart RC, Kennedy J. A New Optimizer using particle swarm theory, *Proceedings of the Sixth International Symposium on Micro Machine and Human Science*, Nagoya: IEEE Press, 39–43, 1995.
11. Dorigo M. *Optimization, Learning and Natural Algorithms*, PhD Thesis, Dipartimento di Elettronica, Politecnico di Milano, IT, 1992.
12. Geem ZW, Kim JH, Loganathan GV, A new heuristic optimization algorithm: Harmony Search, *Simulations*, 2001; **76**: 60–8.
13. McKenna F, Fenves GL. *The OpenSees Command Language Manual* (1.2. edn). PEER, 2001.
14. *Manual of steel construction. Load and resistance factor design*, Chicago, IL: American Institute of Steel Construction; 2001.
15. Vanderplaats GN. *Numerical Optimization Techniques for Engineering Design: With Application*, McGraw-Hill, NewYork, 1984.
16. Salajegheh E, Gholizadeh S. Structural seismic optimisation using meta-heuristics and neural networks: a review, *Comput Tech Rev*, 2012; **5**: 109–37.
17. Farhat F, Nakamura S, Takahashi K. Application of genetic algorithm to optimization of buckling restrained braces for seismic upgrading of existing structures, *Comput Struct*, 2009; **87**: 110–19.
18. Gholizadeh S, Salajegheh E. Optimal design of structures for earthquake loading by self organizing radial basis function neural networks, *Adv Struct Eng*, 2010; **13**: 339–56.
19. Dorigo M, Caro DG, Gambardella LM. Ant algorithms for discrete optimization,

- Artificial Life*, 1999; **5**: 137–72.
20. Luh GC, Lin CY. Structural topology optimization using ant colony optimization algorithm, *Appl Soft Comput*, 2009; **9**: 1343–53.
 21. Kaveh A, Talatahari S. An improved ant colony optimization for the design of planar steel frames, *Eng Struct*, 2010; **32**: 864–73.
 22. Gholizadeh S, Fattahi F. Serial integration of particle swarm and ant colony algorithms for structural optimization, *Asian J Civil Eng*, 2012; **13**: 127–46.
 23. Kaveh A, Ahangaran M. Discrete cost optimization of composite floor system using social harmony search model, *Appl Soft Comput*, 2012; **12**: 372–81.
 24. Gholizadeh S, Barzegar A. Shape optimization of structures for frequency constraints by sequential harmony search algorithm, *Eng Optim*, 2012 (in press).
 25. Degertekin SO. Improved harmony search algorithms for sizing optimization of truss structures, *Comput & Struct*, 2012; **92-93**: 229–41.
 26. Hassan R, Cohanım B, de Weck O, Venter G. A comparison of particle swarm optimization and the genetic algorithm, In: *1st AIAA Multidisciplinary Design Optimization Specialist Conference*. No. AIAA-2005-1897, Austin, 2005.
 27. Li LJ, Huang ZB, Liu F. A heuristic particle swarm optimization method for truss structures with discrete variables, *Comput Struct*, 2009; **87**: 435–43.
 28. Gholizadeh S, Salajegheh E. Optimal design of structures for time history loading by swarm intelligence and an advanced metamodel, *Comput Meth Appl Mech Eng*, 2009; **198**: 2936–49.
 29. Gomes HM. Truss optimization with dynamic constraints using a particle swarm algorithm, *Expert Syst Appl*, 2011; **38**: 957–68.
 30. Gholizadeh S, Fattahi F. Design optimization of tall steel buildings by a modified particle swarm algorithm, *Struct Design Tall Spec Buil*, 2012 (in press).
 31. FEMA-273, NEHRP guideline for the seismic rehabilitation of buildings. Federal Emergency Management Agency, Washington, DC, 1997.
 32. The Language of Technical Computing, MATLAB. Math Works Inc, 2009.